ELSEVIER

Computer Physics Communications 93 (1996) 1-12

Computer Physics Communications

Constructing oscillation preventing scheme for advection equation by rational function

F. Xiao [a], T. Yabe [b], T. Ito [a]

[a] *Department of Electronic Engineering, Faculty of Engineering, Gunma University, 1-5-1 Tenjin Cho, Kiryu, Gunma 376, Japan*

[b] *Department of Energy Sciences, Graduate School at Nagatsuta, Tokyo Institute of Technology, 4259 Nagatsuta, Midori-ku, Yokohama 227, Japan*

Received 10 June 1995; revised 14 September 1995

Abstract

A numerical scheme for solving advection equations is presented. The scheme is derived from a rational interpolation function. Some properties of the scheme with respect to convex-concave preserving and monotone preserving are discussed. We find that the scheme is attractive in suppressing overshoots and undershoots even in the vicinities of discontinuity. The scheme can also be easily switched as the CIP (Cubic interpolated Pseudo-Particle) method to get a third-order accuracy in smooth region. Numbers of numerical tests are carried out to show the non-oscillatory and less diffusive nature of the scheme.

Keywords: Computational algorithm; Advection equation; Rational function; Monotone preserving scheme

1. Introduction

As one of the most important physical processes in fluid dynamics, advection is conventionally described in terms of a differential equation as a first-order hyperbolic type like

$$\frac{\partial f}{\partial t} + \boldsymbol{u} \cdot \nabla f = 0, \tag{1}$$

with f being the dependent variable and $\boldsymbol{u}$ the velocity.

The CIP method, a sophisticated method for the advection equation, has been under development since the middle of the 1980s. It has been applied to simulations of various physical problems and proved to be well performing [1-4]. The rudimentary principle of the CIP, which makes the scheme quite different from other advection solvers, is to treat the spatial derivatives of the interpolation function, which serves as free parameters in the interpolating procedure, as dependent variables. These additional variables are then calculated by their governing equation derived by applying a differential operation to the advection equation with respect to spatial independent variables. Hence, the free parameters needed in interpolation are determined from the given differential equation rather than from combinations of the values at discretised grid knots as those, for example, done with the Akima or Cubic Bessel formula [5].

SSDI 0010-4655(95)00124-7

In practical implementation, an attractive advection scheme should be both less diffusive and oscillation free. Many high order schemes have been proposed to reduce the numerical diffusion. However, in the presence of discontinuity or breaking down of smoothness, one is likely to meet overshoots or undershoots by directly applying those high order methods. On the other hand, we often encounter situations where the property of positivity appears to be of most importance. Algorithms which can preserve the topological nature of data are of particular interest. Usually, as applications of a high order scheme, manipulations, such as numerical viscosity, are made to degrade the scheme to be of lower order in the presence of discontinuities to eliminate spurious oscillation. Some of these sort schemes are reviewed in [6].

In constructing a CIP-type scheme, the choice of interpolation function is of great importance, and some improvements can be expected by using some prospective interpolation functions. We can hope to construct schemes with some desired properties, like TVD, monotone or non-oscillatory, by making use of a proper function.

In this paper, we present an algorithm for the advection equation by employing a rational function. The remarkable character of the scheme is convex-concave preserving and monotone preserving. It makes this method quite desirable for practical implementations where the break-down of positivity from numerically spurious oscillation tends to cause serious problems in calculations or simulated results. The scheme appears also less diffusive in sample calculations.

In Section 2, the algorithm is presented and some related properties are discussed. Numbers of numerical tests are given in Section 3, and a brief conclusion follows in Section 4.

2. The algorithm

For given data $f(x_1), f(x_2), \ldots, f(x_i), \ldots, f(x_{\text{imax}})$ with $x_1 < x_2 < \cdots < x_i < \cdots < x_{\text{imax}}$, we construct a piecewise interpolation function $F_i(x)$ to $f(x)$ by limiting the number of free parameters to be 4 on each interval $[x_i, x_{i+1}]$.

The ith function piece $F_i(x)$ is made to satisfy the continuity condition

$$\begin{cases} F_i(x_i) = f(x_i), & F_i(x_{i+1}) = f(x_{i+1}), \\ F_i'(x_i) = d_i, & F_i'(x_{i+1}) = d_{i+1}, \end{cases} \quad i = 1, 2, \ldots, \text{imax}, \tag{2}$$

where $\{d_i\}$ are free parameters used to evaluate the derivatives of the interpolation function $F(x)$ and can be determined by various formula. In the CIP method, $\{d_i\}$ are calculated from a governing relation derived from the original advection equation, and we will use the same concept in this paper.

Our scheme is derived from a piecewise rational function in a form as

$$F_i(x) = R_i(x) = \frac{f(x_i) + A1_i(x - x_i) + A2_i(x - x_i)^2}{1 + B_i(x - x_i)}. \tag{3}$$

From condition (2), one reads

$$\begin{cases} A1_i = d_i + f_i B_i, \\ A2_i = S_i B_i + (S_i - d_i)\Delta_i^{-1}, \\ B_i = [(S_i - d_i)/(d_{i+1} - S_i) - 1]\Delta_i^{-1}, \end{cases}$$

where

$$\begin{cases} \Delta_i = x_{i+1} - x_i, \\ S_i = (f_{i+1} - f_i)\Delta_i^{-1}, \\ d_i = \left(\dfrac{df}{dx}\right)_i. \end{cases}$$

When $d_i \le S_i \le d_{i+1}$ or $d_i \ge S_i \ge d_{i+1}$ is not satisfied, $B_i \le -\Delta_i^{-1}$ in (3) is observed, and computation will be broken as the denominator of (3) approaches zero at a point within $[x_i, x_{i+1}]$. Thus, for implementation, we modify (3) as

$$F_i(x) = \frac{f(x_i) + A1_i(x - x_i) + A2_i(x - x_i)^2 + A3_i(x - x_i)^3}{1 + \alpha B_i(x - x_i)} \tag{4}$$

and

$$\begin{cases} A1_i = d_i + f_i \alpha B_i, \\ A2_i = S_i \alpha B_i + (S_i - d_i)\Delta_i^{-1} - A3_i \Delta_i, \\ A3_i = [d_i - S_i + (d_{i+1} - S_i)(1 + \alpha B_i \Delta_i)]\Delta_i^{-2}, \\ B_i = [|(S_i - d_i)/(d_{i+1} - S_i)| - 1]\Delta_i^{-1}, \end{cases} \tag{5}$$

$\alpha \in [0, 1]$ is a switching parameter. The new term $A3_i(x - x_i)^3$ is determined in such a way that $A3_i$ vanishes for $(S_i - d_i)/(d_{i+1} - S_i) \ge 0$ with $\alpha = 1$ and recovers the coefficient of $(x - x_i)^3$ term in a cubic interpolation function [1], i.e. $A3_i = (d_i + d_{i+1} - 2S_i)\Delta_i^{-2}$, for $\alpha = 0$.

We write the one-dimensional form of the advection Eq. (1) as

$$\frac{\partial f}{\partial t} + u\frac{\partial f}{\partial x} = 0. \tag{6}$$

The equation governing $\partial f/\partial x$ can be derived directly from Eq. (6) as

$$\partial_t(\partial_x f(x,t)) + u\partial_x(\partial_x f(x,t)) = -\partial_x u(x,t)\partial_x f(x,t), \tag{7}$$

where ∂_x refers to $\partial/\partial x$ and ∂_t to $\partial/\partial t$.

Usually, it is convenient to handle the right hand side of (7) in non-advection phase like the treatment in the CIP which solves equations by time splitting into advection and non-advection phases. Thus then, in advection phase, Eq. (6) and

$$\partial_t(\partial_x f(x,t)) + u\partial_x(\partial_x f(x,t)) = 0 \tag{8}$$

need to be dealt with.

When f_i^n and $\partial_x f_i^n$ are known for $i = 1, \ldots, i_{max}$, with n denoting the time steps, coefficients $A1_i, A2_i, A3_i$ and B_i can be calculated by (5), and then both f_i^{n+1} and $\partial_x f_i^{n+1}$ may be predicted by shifting along the characteristics as

$$f_i^{n+1} = F_i(x_i - u\Delta t) = \frac{f_i^n + A1_i\xi + A2_i\xi^2 + A3_i\xi^3}{1 + \alpha B_i \xi} \tag{9a}$$

and

$$\begin{aligned} \partial_x f_i^{n+1} &= \partial_x F_i(x_i - u\Delta t) \\ &= (A_i + 2A2_i\xi + 3A3_i\xi^2)(1 + \alpha B_i\xi)^{-1} - \alpha B_i(f_i^n + A1_i\xi + A2_i\xi^2 + A3_i\xi^3)(1 + \alpha B_i\xi)^{-2}, \end{aligned} \tag{9b}$$

where $\xi = -u\Delta t$. Eq. (9) is derived for $u \le 0$. When $u > 0$, we need only take the places of Δ_i and $i + 1$ by $-\Delta_{i-1} = x_{i-1} - x_i$ and $i - 1$ in foregoing expressions respectively.

Next, let us state and prove some facts about algorithm (9). By keeping in mind that the scheme is a sort of upwind, without losing generality, we limit our discussions to the case of $u \le 0$.

Proposition 2.1. When the switching parameter α is set zero, algorithm (9) is identical to the CIP method.

Proof. The proof is straightforward by eliminating the terms including α in (9) and comparing the resulting expression with Eq. (3) in Ref. [1]. □

From Proposition 2.1, we know that the CIP method is a particular case of algorithm (9). By letting $\alpha = 0$, the scheme can be switched to the CIP of the third-order in smooth region. Furthermore, one can recover the first-order upwind scheme by setting $d_i^n = d_{i+1}^n = S_i^n$ instead of (9b). Algorithm (9) provides us a flexible form for a class of polynomial based schemes.

Pertaining to the interpolation function itself, we have

Lemma 2.1. Assuming $\alpha = 1$, the interpolation function defined with (3) is retrieved from that defined with (4) if the condition of $d_i \le S_i \le d_{i+1}$ or $d_i \ge S_i \ge d_{i+1}$ is satisfied.

Proof. The proof is trivial because the coefficient $A3_i$ vanishes for the addressed condition. □

Lemma 2.2. Under the condition of Lemma 2.1, we have $F_i''(x) \ge 0$ for $d_i \le d_{i+1}$ and $F_i''(x) \le 0$ for $d_i \ge d_{i+1}$ in every closed subinterval of $[x_i, x_{i+1}]$.

Proof. With Lemma 2.1, by considering function $F_i(x)$ defined with (3), we easily arrive at

$$F_i''(x) = \frac{2(d_{i+1} - S_i)^2 (S_i - d_i)^2 (x - x_i)^2}{[(d_{i+1} - S_i)(x_{i+1} - x) + (S_i - d_i)(x - x_i)]^3}.$$

It states that $F_i''(x) \ge 0$ is always true for $d_i \le S_i \le d_{i+1}$, and $F_i''(x) \le 0$ for $d_i \ge S_i \ge d_{i+1}$. □

We, for further discussion, note some concepts as

Definition 2.1. The data $\{(x_i, f_i, d_i), i = 1, 2, \ldots, \text{imax}\}$ are said to be non-decreasing if $f_1 \le f_2 \le \cdots \le f_{\text{imax}}$ or non-concave if $d_1 \le S_1 \le d_2 \le S_2 \le d_3 \le \cdots \le d_{\text{imax}-1} \le S_{\text{imax}-1} \le d_{\text{imax}}$; or conversely they are said to be non-increasing if $f_1 \ge f_2 \ge \cdots \ge f_{\text{imax}}$ or non-convex if $d_1 \ge S_1 \ge d_2 \ge S_2 \ge d_3 \ge \cdots \ge d_{\text{imax}-1} \ge S_{\text{imax}-1} \ge d_{\text{imax}}$.

Definition 2.2. Let a scheme for Eq. (6) be in a form as

$$f^{n+1} = \Re 1(\Delta t, \Delta, f^n, d^n),$$

and

$$d^{n+1} = \Re 2(\Delta t, \Delta, f^n, d^n),$$

with $f^n = \{f_i^n\}$, $d^n = \{d_i^n\}$ and $\Delta = \{\Delta_i\}$. It is said to be convex-concave preserving if

$$d_1^{n+1} \le d_2^{n+1} \le \cdots \le d_{\text{imax}}^{n+1}$$

is always true for given non-concave data $\{(x_i, f_i^n, d_i^n)\}$, or

$$d_1^{n+1} \ge d_2^{n+1} \ge \cdots \ge d_{\text{imax}}^{n+1}$$

for non-convex data $\{(x_i, f_i^n, d_i^n)\}$;

It is said to be monotone preserving if

$$f_1^{n+1} \le f_2^{n+1} \le \cdots \le f_{\text{imax}}^{n+1}$$

is always true for given non-decreasing data, or

$$f_1^{n+1} \geq f_2^{n+1} \geq \cdots \geq f_{\text{imax}}^{n+1}$$

for non-increasing data.

The scheme is said to be non-oscillatory if there exists

$$0 \leq \frac{f_i^{n+1} - f_i^n}{f_{i+1}^n - f_i^n} \leq 1, \quad i = 1, 2, \ldots, \text{imax}.$$

About the monotone and convex-concave preserving properties of a given scheme, we address an obvious fact as

Lemma 2.3. A scheme for linear advection equation is monotone preserving for non-increasing data if it is monotone preserving for non-decreasing data; and similarly, a scheme is convex-concave preserving for non-concave data if it is convex-concave preserving for non-convex data.

Proof. The proof can be constructed by considering another data set generated as $\{(x_i, p_i = C - f_i), i = 1, 2, \ldots, \text{imax}\}$, where $\{f_i\}$ is the original profile and $C \in \mathbb{R}$ a real constant. $\{p_i\}$ has opposite properties in monotonicity and convexity to $\{f_i\}$, and a solution for $\{p_i\}$ is equivalent to that for $\{f_i\}$ in sense of the transformation. □

Now, with respect to algorithm (9), we can give the following results.

Proposition 2.2. Let $\alpha = 1$, under the CFL condition, i.e. $\xi \leq \Delta$, scheme (9) is convex-concave preserving.

Proof. (i) For non-concave data $\{(x_i, f_i^n, d_i^n), i = 1, 2, \ldots, \text{imax}\}$, there exists $d_i^n \leq S_i^n \leq d_{i+1}^n$. By (9b), $\{d_i\}$ are advanced as $d_i^{n+1} = F_i'(x_i + \xi)$. From Lemma 2.2, and noticing that $F_i'(x_i) = d_i^n \leq F_i'(x_{i+1}) = d_{i+1}^n$, we find that $F_i'(x)$ reaches its minimum at $x = x_i$ and maximum at $x = x_{i+1}$. Since the CFL condition can be interpreted as $x_i \leq x_i + \xi \leq x_{i+1}$, we obtain the convex-concave preserving property as the following inequality:

$$d_i^n \leq d_i^{n+1} \leq d_{i+1}^n.$$

(ii) For non-convex data, we get the result directly by recalling Lemma 2.3. □

Proposition 2.3. Let $\alpha = 1$, under the CFL condition, scheme (9) is non-oscillatory if the given data $\{(x_i, f_i^n, d_i^n)\}$ satisfies anyone of the following:

- $0 \leq d_i^n \leq S_i^n \leq d_{i+1}^n$ (non-decreasing and non-concave),
- $d_i^n \geq S_i^n \geq d_{i+1}^n \geq 0$ (non-decreasing and non-convex),
- $d_i^n \leq S_i^n \leq d_{i+1}^n \leq 0$ (non-increasing and non-concave),
- $0 \geq d_i^n \geq S_i^n \geq d_{i+1}^n$ (non-increasing and non-convex).

Proof. The situation of $S_i^n = 0$ is trivial. We only consider that of $S_i^n \neq 0$. From Lemma 2.1 and (9), we have

$$\begin{aligned} \bar{r}_i \equiv \frac{f_i^{n+1} - f_i^n}{f_{i+1}^n - f_i^n} &= \frac{1}{(1 + B_i\xi) S_i^n \Delta_i} (d_i^n \xi + A1_i \xi^2) \\ &= \frac{1}{(1 + B_i\xi) S_i^n \Delta_i} \left[d_i^n \xi + S_i^n B_i \xi^2 + \frac{(S_i^n - d_i^n)}{\Delta_i} \xi^2 \right]. \end{aligned}$$

(i) For the case of non-decreasing and non-concave data ($0 \leq d_i^n \leq S_i^n \leq d_{i+1}^n$), we know that $S_i^n - d_i^n \geq 0$, and then by CFL condition, get $(S_i^n - d_i^n)\xi^2/\Delta_i \leq (S_i^n - d_i^n)\xi$. Therefore,

$$\bar{r}_i \le \frac{1}{(1+B_i\xi)S_i^n\Delta_i}[S_i^n\xi(1+B_i\xi)] = \frac{\xi}{\Delta_i} \le 1,$$

meanwhile

$$\bar{r}_i = \frac{d_i^n(1-\xi/\Delta_i)\xi + (1+\Delta_i B_i)S_i^n\xi^2/\Delta_i}{(1+B_i\xi)S_i^n\Delta_i}.$$

From $d_i^n \ge 0$ and CFL condition, we get

$$\bar{r}_i \ge \frac{1+B_i\Delta_i}{1+B_i\xi}(\xi/\Delta_i)^2.$$

By (5), one knows that $1+B_i\Delta_i = |(S_i^n - d_i^n)/(d_{i+1}^n - S_i^n)| \ge 0$ and $1+B_i\xi = |(S_i^n - d_i^n)/(d_{i+1}^n - S_i^n)|\xi/\Delta_i + (1-\xi/\Delta_i) \ge 0$, and consequently $\bar{r}_i \ge 0$.

(ii) For the case of non-decreasing and non-convex data ($d_i^n \ge S_i^n \ge d_{i+1}^n \ge 0$), by $S_i^n - d_i^n \le 0$ and CFL condition, we get $(S_i^n - d_i^n)\xi^2/\Delta_i \ge (S_i^n - d_i^n)\xi$, and then

$$\bar{r}_i \ge \frac{1}{(1+B_i\xi)S_i^n\Delta_i}[S_i^n\xi(1+B_i\xi)] = \frac{\xi}{\Delta_i} \ge 0.$$

On the other hand, $\bar{r}_i$ can be rewritten as

$$\bar{r}_i = 1 + \frac{d_{i+1}^n}{S_i^n}(\xi/\Delta_i - 1) + \frac{(d_{i+1}^n - S_i^n)(1-\xi/\Delta_i)^2}{(1+B_i\xi)S_i^n}.$$

Noticing $d_i^n \ge S_i^n \ge d_{i+1}^n \ge 0$ and the CFL condition as well, one finds that the last two terms in the above expression are less than 0, and then $\bar{r}_i \le 1$;

(iii) For non-increasing data we have similar inequalities, or we can complete the proof by Lemma 2.3. □

From Proposition 2.3, it is obvious that (9) leads a solution valued between the maximum and minimum within the cell. Thus, no new extremes will be created. As a corollary of Proposition 2.3, we give another fact as

Proposition 2.4. Let $\alpha = 1$, under the CFL condition, scheme (9) is monotone preserving if the given data is non-concave or non-convex.

Above discussions are undertaken with respect to the interval $[x_i, x_{i+1}]$, and we reach results in a sense of piecewise. For making use of the algorithm, one needs to determine $\{d_i\}$ in advance. One of the choices can be as $d_i^0 = S_i^0$, $i = 1, 2, \ldots,$ imax, obviously, the $\{d_i^0\}$ meet the condition of $d_i^0 \le S_i^0 \le d_{i+1}^0$ or $d_i^0 \ge S_i^0 \ge d_{i+1}^0$. As calculation proceeds, the data is adapted to fit a rational function. Due to the properties of convex-concave preserving, a new extremum is suppressed. We can expect a non-oscillatory profile with the scheme.

Among existing schemes, some are also constructed by interpolating procedures. The most representative ones are the MUSCL (monotonic upwind scheme for conservation laws) scheme of Van Leer [7,8] and the PPM (piecewise-parabolic method) scheme of Colella and Woodward [9]. In these scheme, profiles of dependent variable in control volume is computed by interpolation, and the numerical flux at the center of zones can be determined, subject to certain monotonicity constrains. A piecewise linear interpolation formulation is used in the MUSCL method, while in the PPM scheme, which is a higher-order extension of MUSCL algorithm, a parabolic function is employed in each zone. To eliminate oscillation near great gradients, extra steps are introduced to enforce the monotonicity conditions in these schemes. The modifications made on the variable may cause discontinuities at the edges of control volume. In our present scheme, no modification at all is needed

after the interpolation procedure. The oscillationless results of the present scheme stem from the property of the rational function as discussed in Section 2. What we should mention as another advantage of the present scheme which needs no explicit calculation for flux correction is that it can be more easily extended into a full multi-dimensional form.

We compared the performances of the MUSCL, PPM and algorithm (9) in solving the linear propagation of a profile which includes both large gradient and a sharp corner. Fig. 1 shows results of (a) the MUSCL scheme, (b) the PPM scheme and (c) algorithm (9) after 440 steps of calculation with $CFL = 0.2$. Algorithm (9) and the PPM scheme produce more accurate numerical solutions compared with the MUSCL scheme. The PPM method, which gives a good representation of the large gradient, however, makes a flattened plateau around the sharp corner, while the present scheme represents the sharp corner satisfactorily. It is observed that by introducing the derivatives of dependent variable in the computational process, the present scheme is more compact than MUSCL and PPM methods which cover at least three grid nodes in constructing interpolation function. This makes the scheme to give a better fitting around sharp corner turning.

In the next section, we will give out some numerical tests. The non-oscillatory and less diffusive property is stressed even in the case with extremely irregular initial data.

3. Numerical tests

In this section, we present some sample calculations to test algorithm (9) in a completely rational sense. We refer to the scheme (9) with $\alpha = 1$ as 'completely rational'.

Example 3.1. We solve one-dimensional linear initial problems as

$$\frac{\partial f}{\partial t} + \frac{\partial f}{\partial x} = 0, \quad (t,x) \in [0,\infty) \times (-\infty,+\infty),$$
$$f(x,0) = f^0(x), \quad x \in (-\infty,+\infty),$$

with the following initial conditions:
(i)

$$f^0(x) = \sin \pi(x+1),$$

(ii)

$$f^0(x) = \begin{cases} 1, & |x| \le \frac{1}{5}, \\ 0, & \text{others}, \end{cases}$$

(iii)

$$f^0(x) = \begin{cases} -x\sin(3/2\pi x^2), & -1 \le x < -1/3, \\ |\sin(2\pi x)|, & |x| < 1/3, \\ 2x - 1 - \sin(2\pi x)/6, & 1/3 \le x < 1, \\ f^0(x+2). \end{cases}$$

Equally spaced grid points of $\Delta x = 0.02$ and a CFL number of 0.2 are used.

The initial condition (i) is used to demonstrate the accuracy of the scheme in smooth region. For comparison, we include also the result of the first order upwind scheme in Fig. 2. Scheme (9) appears to be highly accurate when applied to smooth data, and no noticeable errors in amplitude are observed. The first order upwind scheme, however, produced a diffused profile due to its low order in accuracy.

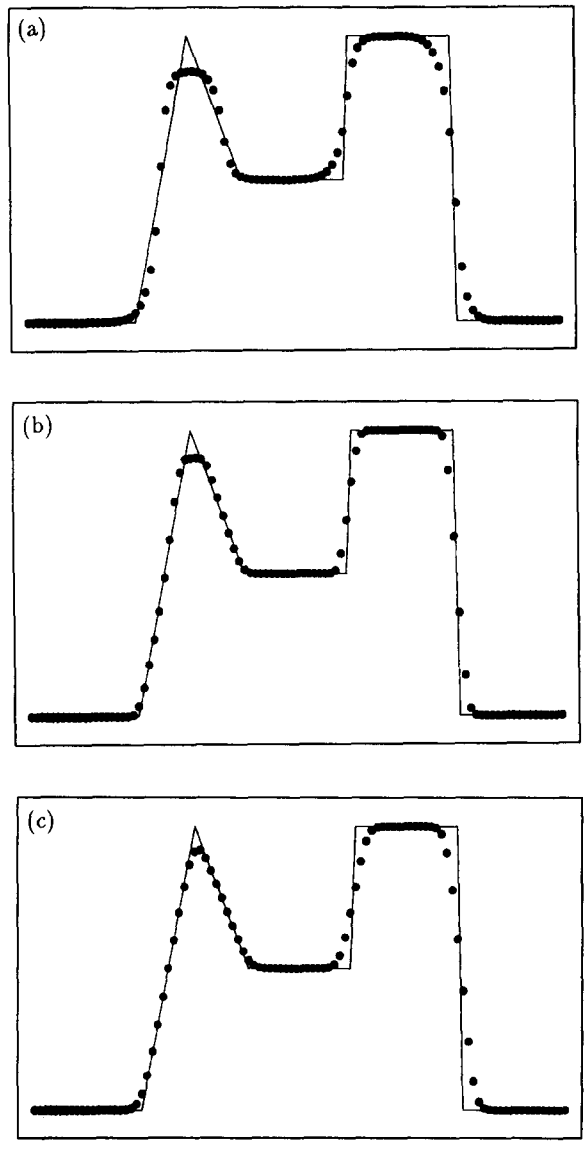

Fig. 1. Linear propagation of a profile including large gradient and sharp corner after 440 time steps ($CFL = 0.2$) with (a) MUSCL scheme of Van Leer, (b) PPM scheme of Colella and Woodward and (c) algorithm (9).

Fig. 3 illustrates the result from condition (ii). We get a non-oscillation solution by directly using (9). In common, high order schemes tend to generate spurious oscillations in the presence of discontinuities or steep gradients, and many modern high resolution scheme use well-specified artificial viscosity to add dissipation near local discontinuities. We fulfill the same task by employing a proper interpolation function.

With condition (iii), we extend the scheme to an extreme case of strong discontinuities, yet the result depicted in Fig. 4 shows a resolution competitive to many prevalent schemes mentioned in Refs. [10] and [11].

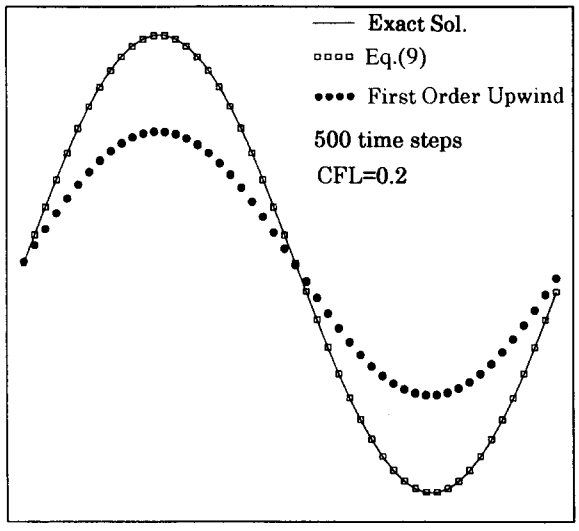

Fig. 2.

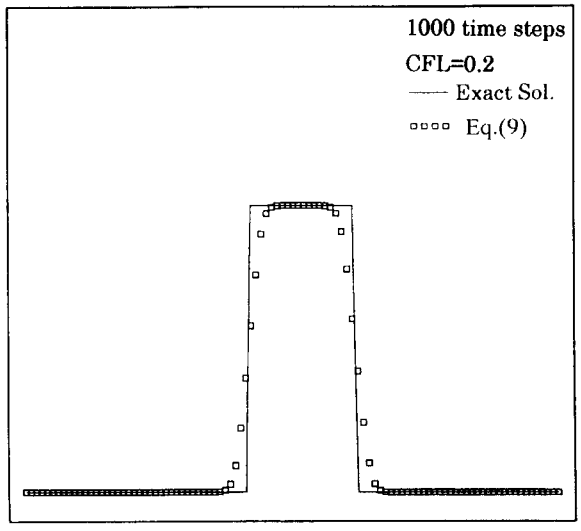

Fig. 3.

Fig. 2. Linear propagation of a sinusoidal wave after 500 time steps ($u \Delta t / \Delta x = 0.2$) with the first-order upwind scheme and the algorithm (9).

Fig. 3. Linear propagation of a square wave after 1000 time steps ($u \Delta t / \Delta x = 0.2$) with the algorithm (9).

Example 3.2. We now turn to a set of two coupled differential equations as

$$\begin{cases} z\dfrac{\partial T_f}{\partial t} + \dfrac{\partial T_f}{\partial x} = T_s - T_f, \\ \dfrac{\partial T_s}{\partial t} = T_f - T_s. \end{cases}$$

It is a two phase model of the dynamic response of porous media and packed beds systems to any inlet temperature. T_f and T_s are dimensionless temperature of fluid and solid respectively, z the heat capacity ratio of fluid to solid, t dimensionless time and x dimensionless spatial coordinate. Interested readers are recommended to refer to [12] and references therein for physical background of the problem.

For a boundary forcing problem, with $-\infty < t < \infty$ and $T_f = (0, t) = g(t)$, one ends up with a solution as

$$T_f(x,t) = e^{-x} g(t - zx) + e^{-x} x^{1/2} \int_0^\infty \tau^{-1/2} e^{-\tau} I_1[2(x\tau)^{1/2}] g(t - zx - \tau) d\tau$$

and

$$T_s(x,t) = e^{-x} \int_0^\infty e^{-\tau} I_0[2(x\tau)^{1/2}] g(t - zx - \tau) d\tau$$

where I_0 and I_1 are the 0th and 1th order modified Bessel function of the first kind.

We calculate the numerical solution to the problem by making use of the first-order upwind difference scheme, Lax–Wendroff scheme and algorithm (9). The time varying function is specified as $g(t) = \cos(\frac{2}{3}\pi t)$ and the heat capacity ratio $z = 9$. A uniform grid system with $\Delta x = 0.025$ is used. The results at $t = 31.5$ are depicted in Fig. 5.

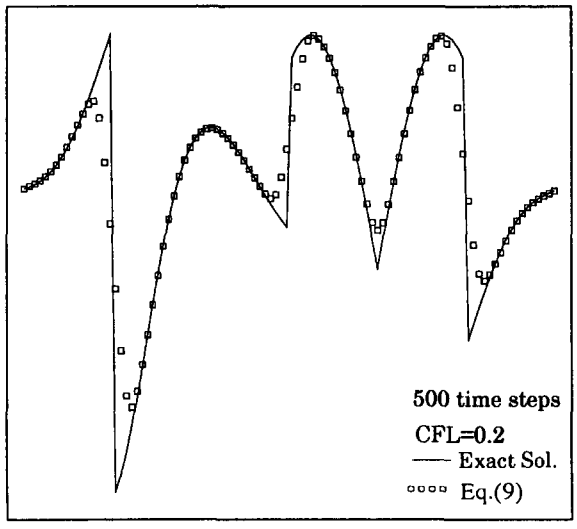

Fig. 4. Linear propagation of a profile given by the initial condition (iii) of Example 3.1 after 500 time steps ($u\,\Delta t/\Delta x = 0.2$) with the algorithm (9).

As a process of propagating and damping boundary perturbation, this sample problem is suitable for testing the errors in amplitude and phase speed for a given advection scheme. The upwind scheme, as expected, gives a heavily diffused solution (Fig. 5a), and few or no variations are observed in the area farther than 3 wave lengths from the forcing source. On the other hand, the Lax–Wendroff scheme appears less encouraging in phase speed. From Fig. 5b, we find an increasing error in phase speed as the distance from forcing source increases, and somewhere the solution takes on a nearly opposite phase compared with the exact one.

Fig. 5c shows the result from (9). No significant errors have been observed in both amplitude and phase speed.

Example 3.3. As an application to non-linear problem, we turn to the one-dimensional shock tube problem which was originally used by G.A. Sod [13],

$$\frac{\partial w}{\partial t} + \frac{\partial f(w)}{\partial x} = 0, \quad (t,x) \in [0,\infty) \times (-\infty,+\infty),$$
$$w(x,0) = w^0(x), \quad x \in (-\infty,+\infty), \tag{10}$$

with the following discontinuous initial conditions:

$$w^0(x) = \begin{cases} w_L, & x \le 0.5, \\ w_R, & x > 0.5. \end{cases}$$

Here $w = (u, \rho u, \rho E)^T$, $f(w) = (\rho u, p + \rho u^2, u(p+E))^T$; ρ is the density, u the velocity, p the pressure, and E the total energy.

For a polytropic gas, there is a relation $p = (\gamma - 1)(E - \frac{1}{2}\rho u^2)$. A numerical test was carried out with $(p_L, \rho_L, u_L) = (1,1,0)$ and $(p_R, \rho_R, u_R) = (0.1, 0.125, 0)$. As done in [1], Eq. (10) was rewritten in a non-conservative form and computational process is divided into advective phase and non-advective phase in terms of (ρ, u, E). An artificial viscosity based on the Rankine–Hugonoit relation in a form like Eq. (29) in [1] was used.

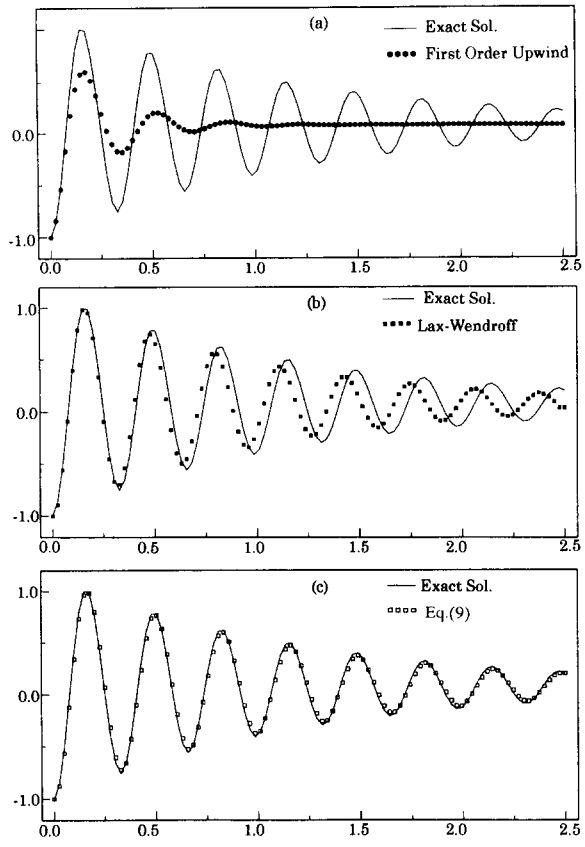

Fig. 5. Dynamic response of a two phase model to a periodical variation of inlet temperature at $t = 31.5$ (a) with the first upwind scheme, (b) with the Lax–Wendroff scheme, (c) with the algorithm (9).

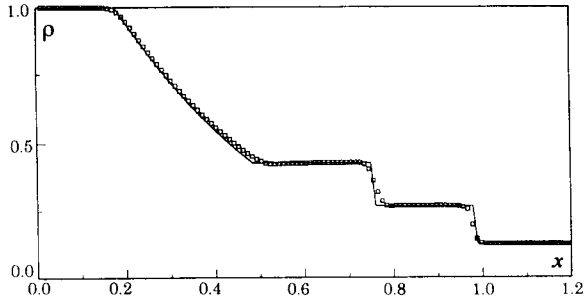

Fig. 6. Density output at $t = 0.277$ of the one-dimensional shock tube problem with the algorithm (9).

The result at $t = 0.277$ is depicted in Fig. 6. We can see, with a proper artificial viscosity as the CIP method, that the present scheme demonstrates ability in capturing both discontinuity and shock wave with a satisfactory accuracy. Compared with the CIP, the scheme (9) tends to produce a less fluctuating solution, even though it appears more diffusive in some senses.

4. Conclusion

We developed a scheme for solving the advection equation by making use of a rational function. Numerical tests and theoretical discussions show that the scheme has a high accuracy in smooth region and no oscillation appears in the vicinities of discontinuities or steep gradients. These properties are commonly desirable for all high resolution schemes. Unlike other high-order schemes, our scheme suppresses spurious oscillation by using a convex-concave preserving interpolation function instead of the flux limiters used in many conventional high resolution schemes. The scheme can reach a high order accuracy in smooth region and produce a 'proper' dissipation in the neighborhood of discontinuity automatically to eliminate numerical oscillation. It is also noted that the CIP method can be easily recovered from the present scheme. Furthermore, the extensions to multi-dimensional version of the scheme is straightforward. Works about 2 and 3 dimensions will be presented in a separate paper.

Acknowledgements

This work was carried out under the collaborating research program at the National Institute for Fusion Science of Japan. Thanks are also extended to Mr. Masato Ida at the Department of Energy Sciences of Tokyo Institute of Technology for helpful discussions.

References

[1] T. Yabe and T. Aoki, Comput. Phys. Commun. 60 (1991) 219.
[2] H. Takewaki and T. Yabe, J. Comput. Phys. 70 (1987) 355.
[3] T. Yabe and T. Ishikawa, P.Y. Wang, T. Aoki, Y. Kadota and F. Ikeda, Comput. Phys. Commun. 66 (1991) 233.
[4] T. Yabe T. Mochizuki and H. Hara, Proceedings of International Conference on Laser Advanced Materials Processing, June 9–12, Nagaoka, Japan (1991).
[5] C. de Boor, A Practical Guide to Splines (Springer, New York, 1987).
[6] H.C. Yee, NASA Report TM-89464 (1987).
[7] B. Van Leer, J. Comput. Phys. 23 (1977) 276.
[8] B. Van Leer, J. Comput. Phys. 32 (1979) 101.
[9] P. Colella and P.R. Woodward, J. Comput. Phys. 54 (1984) 174.
[10] H.M. Wu and S.L. Yang, A Collection of Papers Presented at The Beijing Workshop on Computational Fluid Dynamics (Institute of Mechanics, Academia Sinica, 1990).
[11] C.W. Shu and S. Osher, J. Comput. Phys. 83 (1989) 32.
[12] G. Spiga and M. Spiga, Int. J. Mass Transfer 24 (1981) 355.
[13] G.A. Sod, J. Comput. Phys. 27 (1978) 1.